Peer-reviewed version available at *Viruses* **2019**, *11*, 72; doi:10.3390/v11010072

Review

Monitoring HIV-1 Assembly in Living Cells: Insight from Dynamic and Single Molecule Microscopy

Kaushik Inamdar [1], Charlotte Floderer [1], Cyril Favard [1,*] and Delphine Muriaux [1,*]

[1] IRIM, CNRS UMR9004, CNRS Montpellier, France

* Correspondence: cyril.favard@irim.cnrs.fr; delphine.muriaux@irim.cnrs.fr

Abstract:

HIV-1 assembly is a complex mechanism taking place at the plasma membrane of the host cell. It requires nice spatial and temporal coordination to end up with a full immature virus. Researchers have extensively studied HIV-1 assembly molecular mechanism during the past decades, in order to dissect the respective roles of viral proteins, viral genome and host cell factors. Nevertheless, the time course of the process was observed in living cells only a decade ago. The very recent revolution of optical microscopy, combining high speed and high spatial resolution now permit to study assemblies and their consequences at the single molecule level within (living) cells. In this review, after a short description of these new approaches, we will show how HIV-1 assembly in cells has been revisited using these advanced super resolution microscopy techniques and how much it could make a bridge in studying assembly from the single molecule to the host cell.

Keywords: HIV assembly, SMLM, dynamics

Human Immunodeficiency virus is an enveloped single stranded RNA retrovirus belonging to the family of *Lentiviridae*. It is the causative agent of Acquired Immuno-Deficiency Syndrome (AIDS), estimated to have infected 70 million people since the first reported case with a mortality rate of approximately 50%, and counting today around 37 million people infected worldwide (source WHO 2017). The replication cycle of HIV-1 has been widely studied and characterized. Briefly, HIV-1 infects mainly CD4+ T-lymphocytes by binding to the primary CD4+ receptor via its envelope (Env) protein and fuses by binding to the co-receptors CCR5 or CXCR4 depending on the cell tropism. Post-fusion, uncoating of the virus takes place in the cytoplasm followed by reverse transcription and nuclear import of the viral DNA. Viral DNA integrates into specific sites in the host cell genome and then subverts the host cell machinery to transcribe and translate viral genes into genomes and proteins which are then trafficked to the membrane and assemble into immature virions. Concomitant to the particle release, post-cleavage of the structural Gag proteins by the viral protease occurs to give rise to its mature form and a large structural rearrangement of the viral particle rendering it infectious (for general reviews, see [1,2]).

The HIV-1 Gag structural protein is a 55 kDa polyprotein containing four domains respectively named matrix (MA), capsid (CA), nucleocapsid (NC), and p6, in addition to two small spacer peptides, SP1 and SP2. About ~1500–3000 Gag polyproteins assemble to form a single immature capsid shell [3]. Mutational analyses have revealed that only three domains of Gag (MA, CA, and NC) are required for immature particle assembly, whereas the fourth domain, p6, is required for

budding and release. It is also well known that MA governs membrane targeting. Membrane targeting of Gag requires the N-terminal myristate, as well as residues in MA that form a basic patch (the highly basic region, HBR) and interact with acidic head groups of phospholipids in the PM, including phosphatidylinositol 4,5-bisphosphate (PI(4,5)P2) found in the inner leaflet of the PM [4–12]. CA contains residues that form critical Gag–Gag interactions and NC is required for viral genomic RNA packaging, as well as non-specific interactions with RNA [13], and is essential for particle assembly [14]. Indeed, Gag is the only viral protein required for assembly and release of immature viral particles in cells, although production of infectious virus requires other viral proteins and the genomic RNA.

1. What is known on HIV-1 assembly from classical microscopies?

The mature HIV-1 particle measures 80-150nm in diameter and thus the assembly site is below the resolution limit of conventional optical microscopy methods. Electron microscopy has long been a standard to study HIV-1 assembly, the factors involved therein, and the particle structure [15]. Several studies have used electron microscopy to successfully demonstrate Gag multimerization at the plasma membrane, membrane curvature at the assembly site and viral budding. The role of cellular factors such as the ESCRT machinery in HIV-1 particle release has also been elucidated thanks to this method [16,17]. Scanning and transmission electron microscopy has offered great insights into the formation and morphology of viral particles, providing evidence for electron-dense Gag layers underneath the plasma membrane and nascent particles connected to the cell surface by a thin stalk (for example see [18]). Further advances such as cryo-electron tomography have dropped the resolution to a few angstroms and allow visualisation of viral protein complexes structures close to the atomic level [19–21]. However, despite its stellar contribution to our understanding of HIV-1 particle structures, electron microscopy does not allow the study of the dynamics and the kinetics of nanoscale events taking place during virus assembly at the plasma cell membrane.

The advances of fluorescence microscopy coupled with genetically encoded fluorescence proteins or external fluorophores added on live cells, offered new insights into the dynamics underlying HIV-1 assembly. Ten years ago the introduction of a small Cys rich tag into the viral Gag protein enables the dynamic fluorescent imaging of Gag in model cell lines and in macrophages [22,23]. Since HIV-1 assembly occurs at the plasma membrane of the host cell, most of the improvement in deciphering this process was achieved thanks to the Total Internal Reflexion Fluorescence microscopy (TIRF-M). Kinetics of HIV-1 Gag assembly and particle release could then be visualized for the first time in transfected adherent model cell line [24]. Using live TIRF microscopy, one could observe that Gag associates with the genomic RNA at the cell membrane [25,26], that the 7SL RNA associated with HIV-1 particle [27] and cellular factors, especially ESCRT [25,28,29].. Live TIRF microscopy revealed that Gag molecules that are recruited into assembling particles do so from the rapidly diffusing cytosolic pool, that there is a gradual formation of Gag multimers at the plasma membrane, measured by an increase fluorescent Gag signal at the membrane over time [25,30]. Then multicolor live cell TIRF studies also revealed that membrane targeting by Gag is responsible for anchoring gRNA at the PM [25] and that the recruitment of the ESCRT proteins to enable particle release (ie, bottle neck

Preprints (www.preprints.org) | NOT PEER-REVIEWED | Posted: 26 November 2018 doi:10.20944/preprints201811.0596.v1

Peer-reviewed version available at Viruses 2019, 11, 72; doi:10.3390/v11010072

membrane scission) is sequential [28,31]. Tsg101 is coming first with Gag at the assembly site [28], interacting concomitantly with p6 and NC [32] and persisting, while CHMP and Vps4 proteins comes later and are transient [28,31,33]. The entire process is no longer than 20 minutes and seems to be cell type independent [24,30,34]. It has been extensively reviewed the past 5 years [35,36] but is leaving a black box in between the 5 min of assembly/multimerisation of Gag proteins and the late transient ESCRT arrival and go (Figure 1), where the actin cortical network probably plays an important role as Gag assembling platform stabilization [37]. Using multicolor multifocus TIRF imaging Ivanchenko *et al.* pointed out a possible pre-association of several Gag molecules with the genomic RNA in the cytosol of cells [30]. Later on, using advanced dynamic confocal microscopy techniques such as Raster Image Correlation Spectroscopy (RICS) ([38], Hendrix et al., confirmed the existence of the RNA Gag oligomers in the cytosol of cells [29]. Most of these obtained results are schematized in Figure *1*.

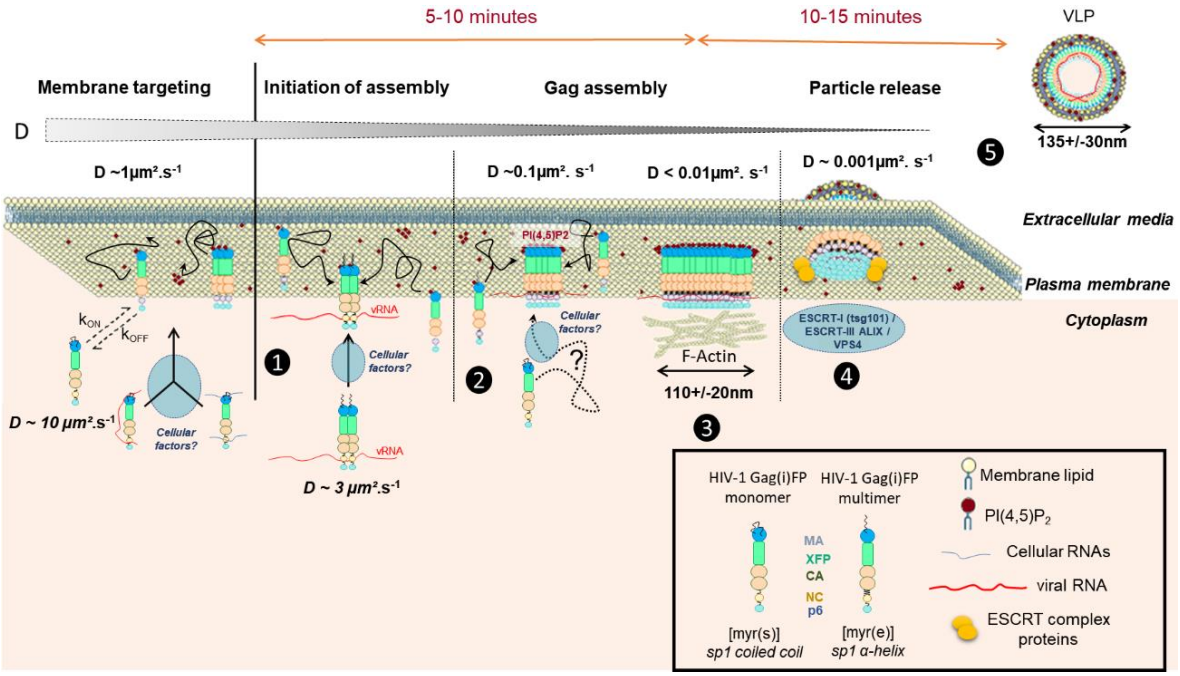

Figure 1: **Scheme of HIV-1 Gag protein dynamics in the cytosol and at the cell plasma membrane during the process of viral particle assembly**. From the left to the right: (1) Cytosolic HIV-1 immature Gag(i)FP tagged protein is coming from the cytosol where it is synthetized, one can measure a diffusion coefficient of 3µm²/s for cytosolic Gag probably as a dimer and already in association with the genomic RNA (vRNA) (from [29,30]). No one knows clearly if any cellular factors are involved at that stage or simple diffusion of Gag targets the cell plasma membrane. (2) Once at the cell membrane, Gag interacts preferentially with acidic lipids, such as PI(4,5)P_2, and anchors the cell membrane through its myristate. Then Gag could dynamically get back to the cytosol (measurable D~3µm²/s) or pursue its multimerization on the viral RNA and at the inner leaflet of the cell PM (measurable Dcoef~1µm²/s) (from [34]), thanks to concomitantly the NC domain-vRNA and the MA-lipid interactions. (3) After 5 min of assembly, ie. Gag multimerization with incorporation of new Gag molecules, 10 minutes are then required before the ESCRT machinery arrival (4)(from [25]), with a very low diffusion coefficient of Gag at the budding site (Dcoef~0.01µm²/s)(from [34]) . During this phase (3), the cortical actin network certainly plays a role in stabilizing the Gag assembly platform (from [37]). (5) Then the immature viral particle (VLP) is released.

Although conventional fluorescence microscopy methods such as wild-field or confocal microscopy have revealed many features of HIV-1 assembly in cells and continue to shed a light on its dynamics, they are severely confined by the diffraction limit (d~250nm), prevented them to access to the molecular details of the assembling virus (d<150nm).

2. Advanced super resolution microscopy shed a light on HIV-1 assembly

In these last two decades, far field optical microscopy has overcome the old resolution barrier -the diffraction limit- enabling visualization of previously invisible molecular details in biological systems. Since their conception, super-resolution imaging methods have continually evolved and can now be used to image cellular structures in three dimensions, with multiple colors, in living systems with nanometer-scale resolution. These methods have been applied to answer questions involving the organization, interaction, stoichiometry, and dynamics of individual molecular building blocks and their integration into functional machineries in cells [39]. Super resolution microscopy (SRM) techniques could be divided into two categories. The first one is based on shaping the illumination light, such as (saturated) structured illumination microscopy (SIM) (resolution increased by 2) and stimulated emission depletion microscopy (STED) (resolution increased by 10). STED involves selective deactivation of fluorophores combine to this illumination shaping to narrow the emission spot down to 20-30 nm [40,41]. The second is based on single-molecule detection and localization (often called single molecule localization microscopy, SMLM) taking advantage of the fluorophore ability to blink or to be photoconverted [42]. In this category are found stochastic optical reconstruction microscopy, STORM [43] and photoactivation localisation microscopy, PALM [44]. These approaches rely upon the acquisition of a set of several thousand images with each image having a random subset of fluorophores stochastically fluorescent at a given time point. By detecting each of single fluorophores and localizing correctly their center of mass, single molecule localizations from each of thousands of images can be obtained. These localizations are then used to reconstruct the final image with single molecule precision.

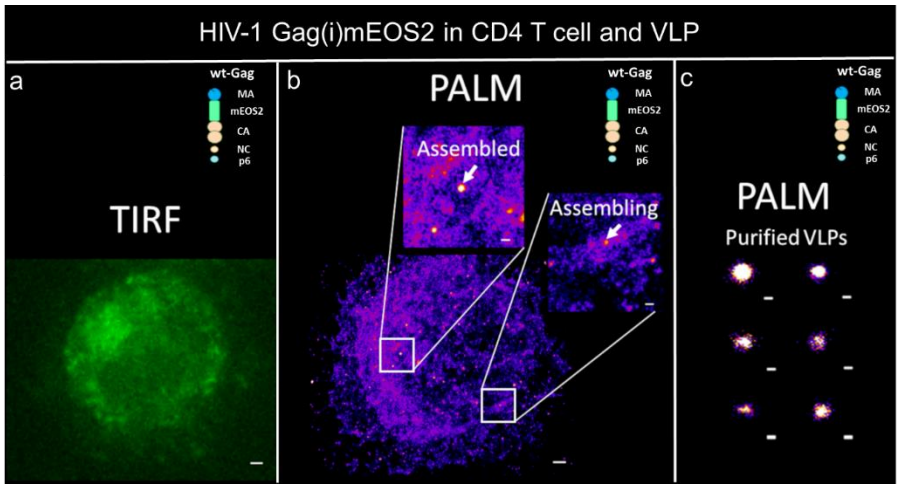

Figure 2 **. A direct comparison of wild-type HIV-1 Gag(i)mEos2 expressing Jurkat CD4 T cell imaging using** (a) **c**lassical TIRF microscopy and (b) Photo Activated Localisation Microscopy (PALM) showing assembling and assembled structures, and (c) HIV-1 immature VLPs. Scale bars are 0.5 μm for a and b, 0.2 μm for b inserts and 0.1μm for c. (adapted from [45,46]).

Benefits from these nanoscale microscopies have been rapidly applied to the study of immature HIV-1 Gag assembly (see Figure 2 for illustration). HIV-1 Gag was one of the first proteins to be visualized by super resolution PALM microscopy [44] showing different cluster sizes of Gag, tagged with mEOS, at the cell plasma membrane of adherent model cell lines (see also Figure 2 in host CD4 T cells). Indeed, single molecule coordinate based analysis shown the existence of three different types of Gag clusters in adherent cells: small random clusters (inferior to 50 nm diameter), clusters of defined size corresponding to assembling sites (between 50 to 130nm) and large patchy aggregations of Gag corresponding to fully assembled structures (~140 nm diameter) [47]. Because the introduction of a protein tag into Gag could play a role, Gunzenhäuser *et al.* compared two photoactivable tags, mEOS2 and tdEOS, with respect to Gag assembly [48]. The results show that Gag tagged with tdEOS forms unusually large clusters as compared to Gag-mEOS2, which in turn forms clusters well within the acceptable range for HIV-1 assembly sites.

Apart from Gag self-assemblies, the formation of an infectious HIV-1 involves viral and cellular factors including other viral proteins, such as Env, the RNA genome and some host cellular proteins in the late steps of HIV-1 assembly and budding. Using 3D SIM imaging, a recent study shows the presence of interacting genomic RNA in the cytosol and its spatial colocalization throughout the cell [49].Several other SRM studies have focused on HIV-1 Env and its dynamics in assembling viral particles. Dual color SRM and dSTORM have illustrated the importance of the CT domain of Env in HIV-1 Gag assembly [50,51]. Mutations in the CT domain of Env resulted in loss of specificity of Env incorporation as revealed by a coordinate based distance distribution n analysis [50]. In addition, image-based morphological cluster analysis demonstrates that Env clusters are larger in presence of assembling virus as compared to EnvΔCT. Roy and coworkers have further demonstrated that Env trimers are already present at the plasma membrane, and that these clusters become significantly larger upon Gag assembly [51].

Studies regarding host cell factors in HIV-1 assembly have mainly focused on the ESCRT machinery. Van Engelenburg *et al.* looked at relative distribution of ESCRT subunits within the budding particle by iPALM and correlative electron microscopy [52]. They showed the initial scaffolding of ESCRT subunits CHMP2A, CHMP4B and TSG101 within the viral bud, the dynamics of which change dramatically on particle release. Furthermore, TSG101, which has been well described to interact with p6 domain of HIV-1 Gag (von Schwedler et al 2003), and recently partially with NC [32], revealed a small cytosolic pool punctuated by localizations within the Gag lattice of assembling particles. Another study revealed a temporal aspect of the recruitment of these subunits in Gag assembly sites as well as the relative localizations in the site [28]. Finally, Prescher and collaborators showed that the membrane scission process is driven from inside the HIV-1 budding neck by ESCRT-III protein assemblies including CHMP4B and CHMP2A while Tsg101 and ALIX which were also located in clusters similar to the dimension of the neck [53].

A few SRM studies have gone further and looked at cell-free virions to detect viral proteins and their positioning within the particle. A STED study in 2012 [54] revealed the distribution of Env on the viral surface was dependent on the maturation process as well as the Env CT domain. Recent correlative iPALM and SEM studies by Pedersen *et al* [55] have opened up the possibilities of SRM to shed light on HIV-1 particle structure.

However, most of the SRM studies, barring a few, were limited to fixed cells imaging and did not extend to elucidate the real-time molecular events occurring in live cells during the HIV-1 assembly process. Nevertheless, one of the main advantages of SRM over electron microscopy is its ability to observe, in real time, ongoing processes at the nanoscale level, making it a technique of choice for studying virus assemblies.

3. Towards a real time molecular description of HIV assembly in living cells.

First attempt to study the spatiotemporal aspect of Gag assembly in living cells was conducted with single particle tracking PALM (sptPALM) [56]. By extracting the diffusion coefficients of each single Gag molecule from their mean square displacement (MSD), Manley *et al.* observed a strong decrease in Gag mobility that was correlated with the presence of Gag clusters on the cell plasma membrane (see Figure 3 and Figure 1). Later on, a comparison of diffusion coefficient distribution enlightened the role of NC-vRNA binding domain of Gag in HIV-1 assembly in adherent cells [57] or in CD4 T-cells [46]. Recently, studies by Floderer *et al.* [34,45] in T cells and Yang *et al.* [58] in adherent cells used sptPALM to track and analyse Gag clusters during assembly and deciphered the role of the viral genomic RNA and the NC domain of HIV-1 Gag in this process. By monitoring the trajectories of single HIV-1 Gag molecules in the vicinity of assembly sites both studies have shown the existence of directed motions towards these assembly sites. Using different Gag mutants, both studies also showed a major role of NC-RNA interaction in HIV-1 assembly at the cell plasma membrane. Indeed, in both cases, it was observed that contrary to the hypothesis that vRNA only functions to drive formation of low-order Gag multimers, there was a crucial dependencies of the full assembly process on NC-RNA interactions. Yang *et al.* [58] classified the Gag trajectories using their mean square displacement and the deviation from the purely diffusive (random) motion by a non-rigorous use of a generalized description of the MSD, using an a>1.3 exponent to consider directed motions from the MSD (see Figure 3 part b, c and d for detailed explanation). In our approach, we used a Langevin description of Gag motions to rigorously disentangle the attractive and the random part of the overall Gag motion. Coupling this with Bayesian inference and Voronoi tessellation [59], we could establish Gag diffusion and attractive energy maps (related to the speed of the directed Gag motions) throughout the entire assembly and budding process for numerous virus like particles at the nanoscale level (see Figure 3, part d). Interestingly, our results strongly suggested that any available cellular RNAs could lead to a complete assembly event with the same attraction energy than the vRNA, i.e. an energy of 3 to 4 kT (2-3 kcal/mol) on average. Interestingly, this energy value is in line with the one measured experimentally *in vitro* for the binding energy of icosahedral viral capsid subunit on the RNA genome (7 kT, [60]). We could also measure that the Gag-Gag interaction mediated by CA-CA dimerization was representing only a third of the Gag attractive energy while the NC-RNA platform represents two third of it [45]. Furthermore, coarse grain modeling predicted recently that the presence of the vRNA lowered the necessary SP1-CA hexameric interaction energy down to 3 kT to achieve correct HIV-1 assembly [61], thus in perfect agreement with our findings in living host T cells (Floderer et al 2018). The capacity to directly measure the energies sensed by Gag during HIV-1 assembly by single molecule microscopy open an incredibly large field of research that can now link coarse grain modeling, *in vitro* quantitative measurements and *in cellulo* experiments.

The spatiotemporal aspects of Env incorporation into HIV-1 virions during particle assembly was also studied recently by Buttler *et al.*, [62] using interferometric PALM (iPALM, [63]). They reported that Env was incorporated in preformed Gag lattices to the neck of the assembling virion, as determined by the Env angular distribution on the surface of cell-associated virus. In parallel, a role of the C-terminal domain of Env in its trapping at the assembly site was elucidated, using sptPALM, by comparing the diffusion of the wt-Env with an Env deficient in the C terminal tail (EnvΔCT). This nanoscale visualization of the budding site could now highlight a possible role of Gag in Env incorporation. Finally, Env mobility in the lipidic membrane of released virion was also studied using another SRM technique, i.e. scanning STED-FCS [64]. Chojnacki *et al.*, reported that Env mobility was really small (10^{-3} $\mu m^2.s^{-1}$) in the virions and constrained by its C-ter domain [65]. This Env mobility was twice increased upon virus maturation. Interestingly the Env diffusion coefficient found in Chojnacki *et al.* [65] is a hundred times smaller than the one observed by Buttler *et al.* [62], leaving an open window regarding the exact process and dynamic of Env incorporation during HIV-1 assembly.

In conclusion, the advanced super resolution microscopies are nowadays opening an incredible field of avenues to revisit some aspects of virology looking at the extreme small (below 100nm) with the possibility of coupling it to live cell imaging. This will enable to decipher virus life cycle in the host cell at the level of the single molecule and spatiotemporally offering a 3D+t view of the events which was not possible 10 years ago.

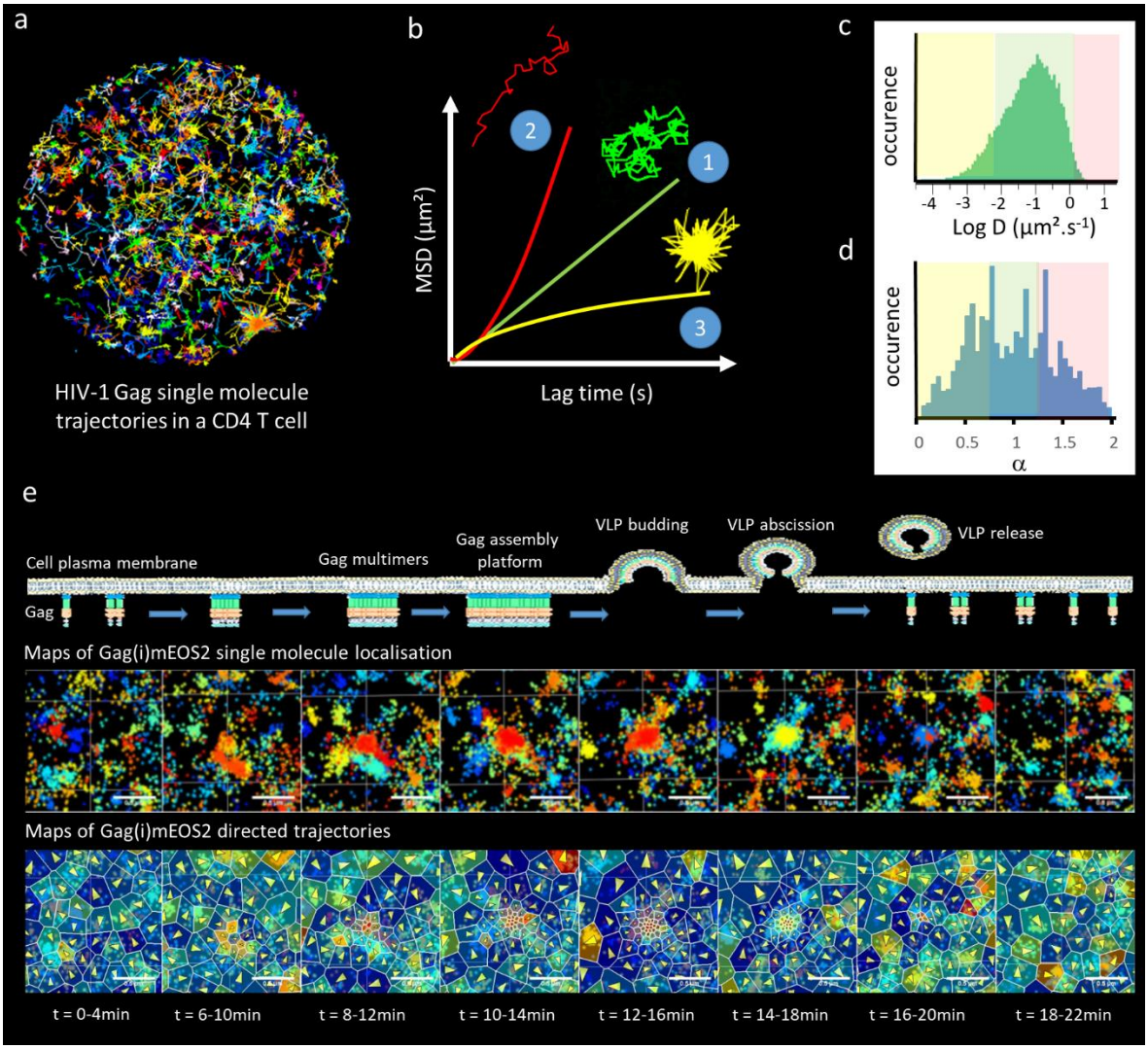

Figure 3 : **Single Gag molecule dynamics during HIV-1 assembly.** a- Trajectories of numerous single Gag observed by TIRF-sptPALM Jurkat T-cells. b - 3 classes of trajectories can be isolated, corresponding either to pure Brownian motion (1, green track), directed motion (2, red track) confined or trapped motion (3, yellow track). By plotting the mean square displacement (MSD) of the single molecule as a function of time, each type of motion could be theoretically distinguished. MSD(t) curves as a function of the motion type (Brownian, green, Directed, red, Confined, yellow) could be non-rigorously approximated by the following relation $MSD(t)=Dt^{\alpha}$ where is an apparent diffusion coefficient and α is either less than 1 (confined motion) or more than 1 (directed motion) with a special case where $\alpha=1$ (Brownian motion) c – Due to noise in the MSD reconstruction it is often difficult to distinguish between confined, Brownian and directed motions, Therefore a simple way to analyze the curves is to fit the MSD(t) with the simple and linear MSD(t)=Dt equation that usually lead to a broad distribution of apparent diffusion coefficients (distribution obtained from the trajectories observed in part a). These apparent diffusion coefficients could for example be arbitrarily divided in each class of motion (yellow, confined, low apparent diffusion coefficient, green Brownian, average apparent diffusion coefficient, red, directed, high apparent diffusion coefficient). d- A less arbitrary method is to fit all the MSD(t) curve with the $MSD(t)=Dt^{\alpha}$ approximation and take benefit of numerous noisy curves to establish statistically relevant distribution of motion, allowing to qualitatively classify the type of motion observed in the cell. This technique has been used to observe directed motion close to the assembly site in [58]. e- A more rigorous analysis aims at disentangling the part of Brownian and directed motion in the trajectory using the Langevin equation of motion. This approach coupled to spatial tesselation, allowed to generate maps of directed motions containing the

average direction as well as the strength of the attraction force generating these directed motions. By coupling this information to the changes in the density of single Gag localization over time, we monitored the attractive energy sensed by each single Gag molecule at the vicinity of HIV-1 assembly site in host CD4 T cells [45].

Author Contributions:

KI, CF and DM wrote and edited the text. CFM draw figure 1. DM and CF composed figure 2 and 3.

Funding: "This research was funded by an ANRS grant, number ECTZ37578" and "KI was funded by associated ANRS PhD fellowship for 3 years (2017-2020)".

Acknowledgments: We would like to thanks the CNRS, the University of Montpellier, and the MRI and Cemipai microscopy facilities at CNRS Montpellier France and the national CNRS consortium GDR IMABIO.

Conflicts of Interest: The authors declare no conflict of interest.

References

1. Muriaux D, Darlix JL, Cimarelli A (2004) Targeting the assembly of the human immunodeficiency virus type I. *Curr Pharm Des* 10(30):3725–3739.

2. Waheed AA, Freed EO (2012) HIV type 1 Gag as a target for antiviral therapy. *AIDS Res Hum Retroviruses* 28(1):54–75.

3. Briggs JAG, et al. (2004) The stoichiometry of Gag protein in HIV-1. *Nature structural & molecular biology* 11:672–675.

4. Charlier L, et al. (2014) Coarse-grained simulations of the HIV-1 matrix protein anchoring: revisiting its assembly on membrane domains. *Biophysical journal* 106(3):577–585.

5. Chukkapalli V, Ono A (2011) Molecular determinants that regulate plasma membrane association of HIV-1 Gag. *J Mol Biol* 410(4):512–524.

6. Chukkapalli V, Hogue IB, Boyko V, Hu W-S, Ono A (2008) Interaction between the Human Immunodeficiency Virus Type 1 Gag Matrix Domain and Phosphatidylinositol-(4,5)-Bisphosphate Is Essential for Efficient Gag Membrane Binding. *J Virol* 82(5):2405–2417.

7. Hamard-Peron E, Muriaux D (2011) Retroviral matrix and lipids, the intimate interaction. *Retrovirology* 8:15.

8. Mercredi PY, et al. (2016) Structural and Molecular Determinants of Membrane Binding by the HIV-1 Matrix Protein. *Journal of molecular biology* 428(8):1637–1655.

9. Olety B, Ono A (2014) Roles played by acidic lipids in HIV-1 Gag membrane binding. *Virus Research* 193:108–115.

10. Ono A, Ablan SD, Lockett SJ, Nagashima K, Freed EO (2004) Phosphatidylinositol (4,5) bisphosphate regulates HIV-1 Gag targeting to the plasma membrane. *Proc Natl Acad Sci USA* 101(41):14889–14894.

11. Saad JS, et al. (2006) Structural basis for targeting HIV-1 Gag proteins to the plasma membrane for virus assembly. *Proc Natl Acad Sci USA* 103(30):11364–11369.

12. Yandrapalli N, et al. (2016) Self assembly of HIV-1 Gag protein on lipid membranes generates PI(4,5)P2/Cholesterol nanoclusters. *Scientific reports* 6:39332.

13. Comas-Garcia M, Davis SR, Rein A (2016) On the Selective Packaging of Genomic RNA by HIV-1. *Viruses* 8(9). doi:10.3390/v8090246.

14. Muriaux D, Darlix J-L (2010) Properties and functions of the nucleocapsid protein in virus assembly. *RNA biology* 7:744–753.

15. Briggs JAG, Kräusslich H-G (2011) The Molecular Architecture of HIV. *Journal of Molecular Biology* 410(4):491–500.

16. Lippincott-Schwartz J, Freed EO, van Engelenburg SB (2017) A Consensus View of ESCRT-Mediated Human Immunodeficiency Virus Type 1 Abscission. *Annu Rev Virol* 4(1):309–325.

17. von Schwedler UK, et al. (2003) The protein network of HIV budding. *Cell* 114(6):701–713.

18. Gelderblom HR, et al. (1988) Fine structure of human immunodeficiency virus (HIV), immunolocalization of structural proteins and virus-cell relation. *Micron and Microscopica Acta* 19(1):41–60.

19. Bharat TAM, et al. (2012) Structure of the immature retroviral capsid at 8 Å resolution by cryo-electron microscopy. *Nature* 487(7407):385–389.

20. Schur FKM, et al. (2015) Structure of the immature HIV-1 capsid in intact virus particles at 8.8 Å resolution. *Nature* 517(7535):505–508.

21. Schur FKM, et al. (2016) An atomic model of HIV-1 capsid-SP1 reveals structures regulating assembly and maturation. *Science* 353(6298):506–508.

22. Gousset K, et al. (2008) Real-time visualization of HIV-1 GAG trafficking in infected macrophages. *PLoS Pathog* 4(3):e1000015.

23. Rudner L, et al. (2005) Dynamic fluorescent imaging of human immunodeficiency virus type 1 gag in live cells by biarsenical labeling. *J Virol* 79(7):4055–4065.

24. Jouvenet N, Bieniasz PD, Simon SM (2008) Imaging the biogenesis of individual HIV-1 virions in live cells. *Nature* 454(7201):236–240.

25. Jouvenet N, Simon SM, Bieniasz PD (2009) Imaging the interaction of HIV-1 genomes and Gag during assembly of individual viral particles. *Proceedings of the National Academy of Sciences of the United States of America* 106:19114–19119.

26. Kemler I, Meehan A, Poeschla EM (2010) Live-cell coimaging of the genomic RNAs and Gag proteins of two lentiviruses. *J Virol* 84(13):6352–6366.

27. Itano MS, Arnion H, Wolin SL, Simon SM (2018) Recruitment of 7SL RNA to assembling HIV-1 virus-like particles. *Traffic* 19(1):36–43.

28. Bleck M, et al. (2014) Temporal and spatial organization of ESCRT protein recruitment during HIV-1 budding. *Proc Natl Acad Sci USA* 111(33):12211–12216.

29. Hendrix J, et al. (2015) Live-cell observation of cytosolic HIV-1 assembly onset reveals RNA-interacting Gag oligomers. *The Journal of cell biology* 210:629–646.

30. Ivanchenko S, et al. (2009) Dynamics of HIV-1 assembly and release. *PLoS pathogens* 5:e1000652–e1000652.

31. Baumgärtel V, et al. (2011) Live-cell visualization of dynamics of HIV budding site interactions with an ESCRT component. *Nat Cell Biol* 13(4):469–474.

32. El Meshri SE, et al. (2018) The NC domain of HIV-1 Gag contributes to the interaction of Gag with TSG101. *Biochim Biophys Acta Gen Subj* 1862(6):1421–1431.

33. Weissenhorn W, Poudevigne E, Effantin G, Bassereau P (2013) How to get out: ssRNA enveloped viruses and membrane fission. *Curr Opin Virol* 3(2):159–167.

34. Floderer C, et al. (2018) Live single molecule microscopy of HIV-1 assembly in host T cells reveals a spatio-temporal effect of the viral genome. *bioRxiv* 10.1101/267930. doi:10.1101/267930.

35. Baumgärtel V, Müller B, Lamb DC (2012) Quantitative live-cell imaging of human immunodeficiency virus (HIV-1) assembly. *Viruses* 4(5):777–799.

36. Jouvenet N, Simon SM, Bieniasz PD (2011) Visualizing HIV-1 assembly. *Journal of molecular biology* 410:501–511.

37. Thomas A, et al. (2015) Involvement of the Rac1-IRSp53-Wave2-Arp2/3 Signaling Pathway in HIV-1 Gag Particle Release in CD4 T Cells. *Journal of virology* 89(16):8162–8181.

38. Digman MA, et al. (2005) Measuring fast dynamics in solutions and cells with a laser scanning microscope. *Biophys J* 89(2):1317–1327.

39. Sahl SJ, Hell SW, Jakobs S (2017) Fluorescence nanoscopy in cell biology. *Nature Reviews Molecular Cell Biology* 18:685.

40. Harke B, et al. (2008) Resolution scaling in STED microscopy. *Optics Express* 16(6):4154.

41. Hell SW, Wichmann J (1994) Breaking the diffraction resolution limit by stimulated emission: stimulated-emission-depletion fluorescence microscopy. *Opt Lett* 19(11):780–782.

42. Ambrose WP, Moerner WE (1991) Fluorescence spectroscopy and spectral diffusion of single impurity molecules in a crystal. *Nature* 349:225.

43. Rust MJ, Bates M, Zhuang X (2006) Sub-diffraction-limit imaging by stochastic optical reconstruction microscopy (STORM). *Nat Methods* 3(10):793–795.

44. Betzig E, et al. (2006) Imaging intracellular fluorescent proteins at nanometer resolution. *Science* 313(5793):1642–1645.

45. Floderer C, et al. (2018) Single molecule localisation microscopy reveals how HIV-1 Gag proteins sense membrane virus assembly sites in living host CD4 T cells. *Scientific Reports* 8(1):16283.

46. Mariani-Floderer C, Sibarita J-B, Favard C, Muriaux DM (2016) Hunting Down HIV-1 Gag Proteins at the Plasma Membrane of Human T Lymphocytes. *AIDS research and human retroviruses* 32(7):658–659.

47. Malkusch S, Muranyi W, Müller B, Kräusslich H-G, Heilemann M (2013) Single-molecule coordinate-based analysis of the morphology of HIV-1 assembly sites with near-molecular spatial resolution. *Histochem Cell Biol* 139(1):173–179.

48. Gunzenhäuser J, Olivier N, Pengo T, Manley S (2012) Quantitative super-resolution imaging reveals protein stoichiometry and nanoscale morphology of assembling HIV-Gag virions. *Nano Lett* 12(9):4705–4710.

49. Ferrer M, et al. (2016) Imaging HIV-1 RNA dimerization in cells by multicolor super-resolution and fluctuation microscopies. *Nucleic Acids Res* 44(16):7922–7934.

50. Muranyi W, Malkusch S, Müller B, Heilemann M, Kräusslich H-G (2013) Super-resolution microscopy reveals specific recruitment of HIV-1 envelope proteins to viral assembly sites dependent on the envelope C-terminal tail. *PLoS Pathog* 9(2):e1003198.

51. Roy NH, Chan J, Lambelé M, Thali M (2013) Clustering and mobility of HIV-1 Env at viral assembly sites predict its propensity to induce cell-cell fusion. *J Virol* 87(13):7516–7525.

52. Van Engelenburg SB, et al. (2014) Distribution of ESCRT machinery at HIV assembly sites reveals virus scaffolding of ESCRT subunits. *Science* 343(6171):653–656.

53. Prescher J, et al. (2015) Super-resolution imaging of ESCRT-proteins at HIV-1 assembly sites. *PLoS Pathog* 11(2):e1004677.

54. Chojnacki J, et al. (2012) Maturation-dependent HIV-1 surface protein redistribution revealed by fluorescence nanoscopy. *Science* 338(6106):524–528.

55. Pedersen M, et al. (2018) Correlative iPALM and SEM resolves virus cavity and Gag lattice defects in HIV virions. *Eur Biophys J*. doi:10.1007/s00249-018-1324-0.

56. Manley S, et al. (2008) High-density mapping of single-molecule trajectories with photoactivated localization microscopy. *Nature methods* 5:155–157.

57. Chen AK, et al. (2014) MicroRNA binding to the HIV-1 Gag protein inhibits Gag assembly and virus production. *Proceedings of the National Academy of Sciences of the United States of America* 111:E2676–E2683.

58. Yang Y, et al. (2018) Roles of Gag-RNA interactions in HIV-1 virus assembly deciphered by single-molecule localization microscopy. *Proc Natl Acad Sci USA* 115(26):6721–6726.

59. El Beheiry M, et al. (2016) A Primer on the Bayesian Approach to High-Density Single-Molecule Trajectories Analysis. *Biophysical journal* 110:1209–1215.

60. Chevreuil M, et al. (2018) Nonequilibrium self-assembly dynamics of icosahedral viral capsids packaging genome or polyelectrolyte. *Nature Communications* 9(1):3071.

61. Pak AJ, et al. (2017) Immature HIV-1 lattice assembly dynamics are regulated by scaffolding from nucleic acid and the plasma membrane. *Proc Natl Acad Sci USA* 114(47):E10056–E10065.

62. Buttler CA, et al. (2018) Single molecule fate of HIV-1 envelope reveals late-stage viral lattice incorporation. *Nat Commun* 9(1):1861.

63. Shtengel G, et al. (2009) Interferometric fluorescent super-resolution microscopy resolves 3D cellular ultrastructure. *Proc Natl Acad Sci USA* 106(9):3125–3130.

64. Honigmann A, et al. (2014) Scanning STED-FCS reveals spatiotemporal heterogeneity of lipid interaction in the plasma membrane of living cells. *Nat Commun* 5:5412.

65. Chojnacki J, et al. (2017) Envelope glycoprotein mobility on HIV-1 particles depends on the virus maturation state. *Nat Commun* 8(1):545.

We would like to apologize for those whom the references were not cited here.